

A High Order Spectral model for wave interaction with a bottom mounted cylinder.

F. Bonnefoy^a R. Eatock Taylor^a P.H. Taylor^a P. Ferrant^b

^aDepartment of Engineering Science, University of Oxford, Parks Road, Oxford OX1 3PJ, UK

^bLaboratoire de Mécanique des Fluides, École Centrale de Nantes, 1 rue de la Noë, BP 92101 44321 NANTES Cedex 3, FRANCE

1 Introduction

The design and operation of large offshore structures requires an accurate estimation of hydrodynamic effects due to waves in various conditions. Due to the nonlinearities in the problem, fully nonlinear models have been used to study the interaction in the time domain, such as boundary element models. However, the models developed so far still tend to be very demanding with respect to computational time. It is then hard to use mesh refinement enabling the study of steep incoming waves.

We address here the development of a fast fully nonlinear numerical model, in the case of a vertical bottom-mounted circular cylinder. The previous work from Dommermuth and Yue [2] and West *et al.* [6] on a High-Order Spectral model in a periodic rectangular domain is applied in cylindrical geometry. The aim is to simulate the time domain evolution of the interaction between the inner cylinder and an incident wave packet. The incident wave packet will be specified later: we focus our attention here on the wave field diffracted by the cylinder. Such an HOS approach, initially developed in a rectangular periodic domain, has been used so far also in rectangular (Le Touzé *et al.* [5], Ducrozet *et al.* [3]) or cylindrical basins (Zhu *et al.* [7]). Alternate approaches have also been considered, such as the Laplacian solver developed by Grue [4].

The formulation is presented as well as linear results as validation of the spectral expansion in the cylindrical domain.

2 Formulation

Potential theory is used to describe the motion of the water surrounding the structure. The flow around the cylinder of radius R is modeled in a circular ring-shaped basin of inner radius R , outer radius $L \gg R$ and finite depth h . The free surface conditions are written in terms of elevation $\eta(\mathbf{x}, t)$ and free surface potential $\phi_s(\mathbf{x}, t) = \phi(\mathbf{x}, \eta(\mathbf{x}, t), t)$ where \mathbf{x} represents the horizontal coordinates (x, y) . These conditions providing the time derivatives of η and ϕ_s , these two variables are time-marched once the vertical velocity W is known. This velocity is approximated by the High Order Spectral method described by Dommermuth and Yue [2] and West *et al.* [6] and adapted to the cylindrical geometry.

Before applying this approximation, the potential is separated into two parts $\phi = \phi^a + \phi^d$ following Agnon and Bingham [1]. The first additional part ϕ^a takes into account the inhomogeneous condition on the inner cylinder. An incident wave field would for example provide a RHS to this condition. The second part ϕ^d has to satisfy homogeneous conditions on the lateral boundaries and is thus suitable for a spectral expansion. The free surface boundary condition can be now written as follows, ready to time march η and ϕ_s^d :

$$\begin{aligned} \frac{\partial \eta}{\partial t} &= -\nabla \eta \cdot \nabla \phi_s^d + (1 + |\nabla \eta|^2) W^d - \nabla \eta \cdot \nabla \phi^a + \frac{\partial \phi^a}{\partial z} \quad \text{for } z = \eta, \\ \frac{\partial \phi_s^d}{\partial t} &= -g\eta - \frac{1}{2} |\nabla \phi_s^d|^2 + \frac{1}{2} [1 + |\nabla(\eta|^2)] (W^d)^2 - \nabla \phi^a \cdot \nabla \phi_s^d - \frac{\partial \phi^a}{\partial t} - \frac{1}{2} |\tilde{\nabla} \phi^a|^2 \quad \text{for } z = \eta, \end{aligned}$$

where $\tilde{\nabla}$ is the gradient and ∇ the horizontal gradient. A damping pressure is added to the dynamic free surface condition. Provided the absorption is efficient, the modeled basin is equivalent to a semi-infinite basin in the

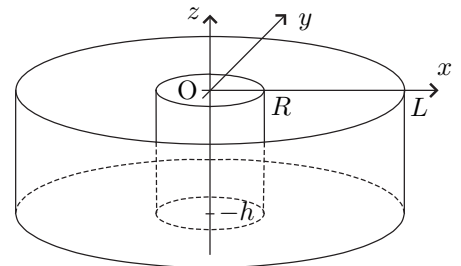


Figure 1: Domain and reference

Email addresses: Felicien.Bonnefoy@eng.ox.ac.uk (F. Bonnefoy), R.EatockTaylor@eng.ox.ac.uk (R. Eatock Taylor), Paul.Taylor@eng.ox.ac.uk (P.H. Taylor), Pierre.Ferrant@ec-nantes.fr (P. Ferrant).

radial direction. This damping term is non-zero only close to the outer boundary and prevents the incoming waves from being reflected towards the cylinder. No such term is added to the kinematic condition to ensure mass conservation.

3 Spectral expansion on the free surface

Within the HOS approximation of the vertical velocity, appear a set of Dirichlet problems for the potential components $\phi^{(m)}$, $m = 1$ to M . The Laplace equation and the homogeneous boundary conditions on the bottom and the cylinders are satisfied by means of a spectral expansion on the natural or eigen modes of the ring-shaped basin. Each component $\phi^{(m)}$ of the potential is thus written as

$$\phi^{(m)} = \sum_{p,n} A_{pn}(t) F_n(k_{pn}r) \cos n \theta \frac{\cosh k_{pn}(z+h)}{\cosh k_{pn}h}$$

where the radial eigen function $F_n(k_{pn}r)$ is a linear combination of the Bessel functions of first and second kind, J_n and Y_n , and satisfies the lateral boundary conditions. The condition on the outer cylinder is satisfied by letting $F_n(kr) = -Y'_n(kL) J_n(kr) + J'_n(kL) Y_n(kr)$, the wavenumbers k_{pn} being thus chosen as the solutions of the characteristic equation $Y'_n(kL) J'_n(kR) + J'_n(kL) Y'_n(kR) = 0$ given by the condition on the inner cylinder (see *e.g.* Wehausen and Laitone). The radial eigen functions are eventually normalised. The modal amplitudes $A_{pn}(t)$ are obtained through the HOS iterative scheme.

4 Numerical aspects

The first task is to compute the zeros of the characteristic equation for each azimuthal mode. The procedure we have adopted consists in starting with good estimates of the zero's range and, then, in using Newton's method to refine their evaluations to the desired machine precision.

A numerical procedure is required to transform the quantities from the physical space to the modal space. The azimuthal direction is treated classically by means of Fourier Transforms. In the radial direction, a Gaussian quadrature is inadequate despite its numerical efficiency. It would lead to a set of unequally spaced grid points for each azimuthal mode whereas the free surface conditions involve products in the physical space and therefore all the quantities must be known at the same grid points. A simpler approach is then considered by evaluating the radial integrals by means of a closed Newton-Cotes formula. A formula of degree 9 is used and the number of equally-spaced grid points is greater than the number of modes to ensure a correct accuracy. The required values of the basis functions at the grid points are evaluated and stored at the beginning of the simulation. As a test of the transform accuracy, we compute the overlap matrices $S_{pq}^n = \langle F_n(k_{pn}r) | F_n(k_{qn}r) \rangle$. The maximum deviation from zero off the diagonal of the matrices is 10^{-7} with 40 radial modes, 32 azimuthal modes and 300 grid points in the radial direction.

5 Additional potentials and spectral expansion

At each time step, one has to evaluate the additional forcing terms in the free surface conditions. As in the rectangular domain, we build an extended domain on which the boundary conditions will lead to a finite set of wavenumbers. Figure 2 shows the process of building this extended domain in three steps. The original basin is shown at the left where the shaded area stands for the bottom. First a plane of symmetry is used at $z = L_{rac}/2$ (the cross on the middle part of figure 2) and the symmetric basin is drawn (middle). The domain is closed by

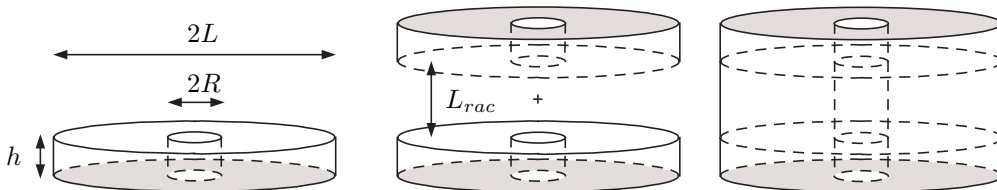


Figure 2: Building the extended domain

a wall at $r = L$ between $z = 0$ and $z = L_{rac}$ (right). The last step is to build the cylinder condition on the

inner cylinder $r = R$. The cylinder condition is first set in the upper basin from the values in the lower basin by point symmetry around the point $z = L_{rac}/2$. This ensure a null average flux on $r = R$. Eventually the cylinder condition is extended between $z = 0$ and $z = L_{rac}$ by a third order polynomial chosen so to keep the extended condition \mathcal{C}^1 continuous between $z = -h$ and $z = L_{rac} + h$.

In this new domain, the additional potential has to satisfy the Laplace equation plus homogeneous conditions on $z = -h$ and $r = L$. This gives a set of eigen modes. The remaining condition on the inner cylinder gives their amplitude. The boundary conditions on $z = -h$ and the point symmetry around $z = L_{rac}/2$ lead to a set of useful wavenumbers

$$K_m = \frac{(2m-1)\pi}{2h + L_{rac}}$$

Subsequently, the eigen functions in the radial direction are built from the modified Bessel functions of first and second kind

$$f_n(K_m r) = -K'_n(K_m L) I_n(K_m r) + I'_n(K_m L) K_n(K_m r) \quad (1)$$

We further normalise the radial mode by a factor $1/K_m L$ so that finally $f_n(K_m L) = 1$. The additional potential is expanded on this basis and can be written as

$$\phi^a = \sum_{m,n} B_{mn}(t) f_n(K_m r) \cos K_m(z+h) \begin{cases} \cos n \theta \\ -\sin n \theta \end{cases} \quad (2)$$

We further need its time derivative in the free surface conditions so we choose to rewrite the condition on the inner cylinder for the time derivative of ϕ^a and include this potential in the time-marching procedure. Through this modified cylinder condition, the modal amplitudes are simply obtained as

$$B'_{mn}(t) = \frac{4}{\pi K_m (2h + L_{rac}) f'_n(K_m R)} \int_{-h}^{L_{rac}/2} dz \int_0^{2\pi} d\theta \left(\frac{\partial^2 \phi^a}{\partial r \partial t} \right)_{r=R} \cos K_m(z+h) \begin{cases} \cos n \theta \\ -\sin n \theta \end{cases}$$

where the second partial derivative represents the time derivative of the RHS of the cylinder condition. The integrals are evaluated by means of Fourier Transforms. The RHS will be provided later by the incident wave field. This coupling has not been implemented yet. At the moment, three RHS have been used so far by moving or deforming gently the cylinder, the velocity being mainly radial. The generic expression of the velocity is $\mathbf{U} = -a\omega \sin(\omega t - n\theta + \psi) \mathbf{u}$ with

- $\mathbf{u} = \mathbf{u}_x$ and $n = 0$ radiation: translation in the horizontal plane
- $\mathbf{u} = \mathbf{u}_r$ and $n = 0$ wave generation by breathing
- $\mathbf{u} = \mathbf{u}_r$ and $n \neq 0$ spiral wave generation

6 First results

Figure 3 shows two examples of free surface elevations obtained with the presented model. Basin dimensions are $R = 1m$, $L = 10m$ and $h = 1m$. On the left the waves are generated by a spiral ($n = 2$) deformation of the cylinder at a 1.5s period. On the right the cylinder oscillates horizontally in the x -direction at a 1.1s period. In both cases, 40×16 modes are used on the free surface and 16×8 on the extended cylinder.

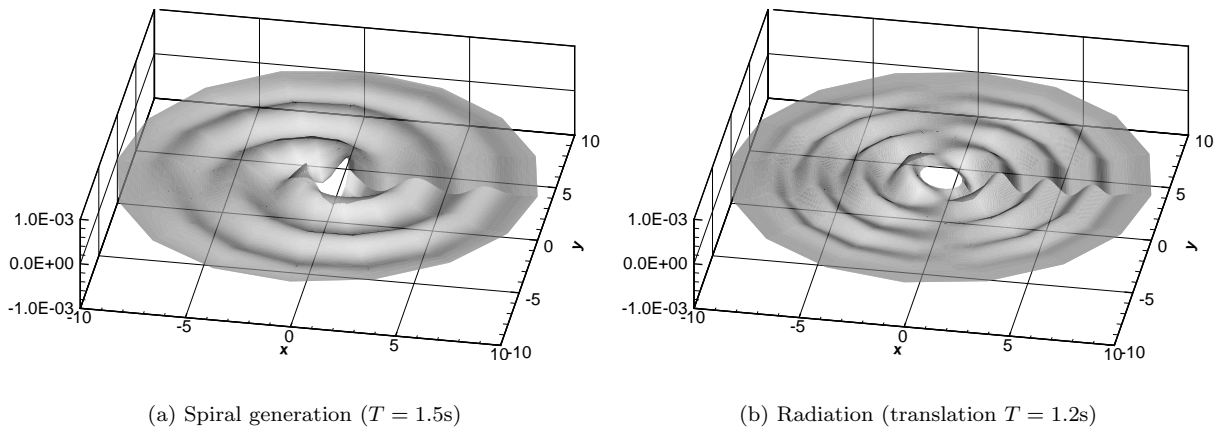


Figure 3: Examples of wave fields

Figure 4 shows the water elevation on the line $\theta = 0$ at $t = 10.2T$ for three different amplitudes of cylinder translation along the x -axis. One can note the increase of the wave height on the cylinder at $r/h = 1$ as the

amplitude increases. Away from the cylinder, the wave field is also modified according to an increase of the phase velocity due to nonlinear effects of third order and higher.

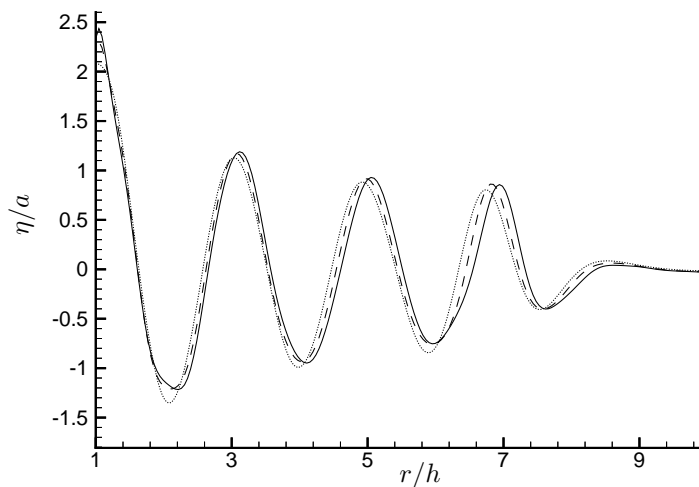


Figure 4: Finite amplitude effects on radiation (dotted $a/h = 4.10^{-4}$, dashed $a/h = 0.04$, solid $a/h = 0.06$)

7 Future work

The aim is to add the external description of an incident wave field. To that extent, the free surface elevation and potential will be rewritten respectively $\eta = \eta^i + \eta^d$ and $\phi = \phi^i + \phi^d + \phi^a$. The incident terms η^i and ϕ^i are specified in alternative ways, either analytical or numerical. They appear in the RHS terms of both the cylinder and free surface conditions.

Numerically, the implementation of the FFTLog approach could lead to faster Transforms in the radial direction leading to a fully $N \log N$ computational cost. Convergence tests will be shown at the conference as well as evaluation of forces on the cylinder.

Acknowledgements

This work has been supported by the Délégation Générale de l'Armement (DGA) of the French Ministry of Defence under post-doctorate funding (0534027).

References

- [1] Yehuda Agnon and Harry B. Bingham. A non-periodic spectral method with applications to non linear water waves. *Eur. J. Mech. B/ Fluids*, 18:527–534, 1999.
- [2] Douglas G. Dommermuth and Dick K.P. Yue. A high-order spectral method for the study of nonlinear gravity waves. *J. Fluid Mech.*, 184:267–288, 1987.
- [3] G. Ducrozet, F. Bonnefoy, D. Le Touzé, and P. Ferrant. Development of a fully nonlinear water wave simulator based on higher order spectral theory. In *Proc. 20th IWWFNB*, Norway, May 2005.
- [4] John Grue. A nonlinear model for surface waves interacting with a surface-piercing cylinder. In *Proc. 20th IWWFNB*, Norway, May 2005.
- [5] D. Le Touzé, F. Bonnefoy, and P. Ferrant. A fully-nonlinear high-order spectral 3d model for gravity waves generation and propagation. In *Proc. 19th IWWFNB*, Italy, March 2004.
- [6] Bruce J. West, Keith A. Brueckner, Ralph S. Janda, D. Michael Milder, and Robert L. Milton. A new numerical method for surface hydrodynamics. *J. Geophys. Res.*, 92(C11):11,803–11,824, October 1987.
- [7] Q. Zhu, Y. Liu, and D. K. P. Yue. Three-dimensional instability of standing waves. *J. Fluid Mech.*, 496:213–242, 2003.